# Supplementary data

## Three novel transition metal complexes of 6-methyl-2-oxo-quinoline-3-carbaldehyde thiosemicarbazone: synthesis, crystal structure, cytotoxicity, and mechanism of action

Bi-Qun Zou[a,b†], Xing Lu[a†], Qi-Pin Qin[a], Yu-Xia Bai[a], Ye Zhang[a,b,c*], Meng Wang[a], Yan-Cheng Liu[a], Zhen-Feng Chen[a,*], Hong Liang[a,*]

**Table S1** Crystallographic data and refinements of complexes **1-2**.

| | | |
|---|---|---|
| Formula | $C_{12}H_{14}N_6O_8SZn$ | $C_{12}H_{16}CuN_6O_9S$ |
| Mr | 467.74 | 483.91 |
| Crystal system | Monoclinic | Triclinic |
| Space group | $P2_1/c$ | P-1 |
| a/Å | 7.633(15) | 8.5965(8) |
| b/Å | 27.01(5) | 10.0815(9) |
| c/Å | 10.461(16) | 12.1404(14) |
| α/° | 90.00 | 110.051(2)° |
| β/° | 125.38(10) | 95.727(1)° |
| γ/° | 90.00 | 90.148(1)° |
| V/Å$^3$ | 1758(5) | 982.69(1) |
| T/K | 296.15 | 298(2) |
| Z | 4 | 2 |
| $D_c$/g.cm$^{-3}$ | 1.767 | 1.635 |
| $\theta$/° | 5.64 to 52.48° | 3.1 to 25.7 |
| $F$ (000) | 952.0 | 494 |
| $\mu$ (Mo, Kα)(mm$^{-1}$) | 1.573 | 1.28 |
| Total no. reflns | 1637 | 5102 |
| No. indep. reflns | 891 | 3365 |
| $R_{int}$ | 0.0481 | 0.058 |
| R1 [I＞2σ (I)] | 0.1133 | 0.169 |
| ωR2(all data) | 0.3252 | 0.454 |
| Gof($F^2$) | 1.431 | 1.71 |

**Table S2** Selected bond lengths (Å) and angles (°) for complex **1**.

| Bond names | Bond length(Å) | Bond angle | Angle(°) |
|---|---|---|---|
| Cu(1)—O(1) | 1.926(13) | O(1)—Cu(1)—N(1) | 90.5(6) |
| Cu(1)—N(1) | 1.970(14) | O(1)—Cu(1)—N(1′) | 90.5(6) |
| Cu(1)—N(1′) | 1.992(16) | N(1)—Cu(1)—N(1′) | 168.4(6) |
| Cu(1)—O(3′) | 2.17(3) | O(1)—Cu(1)—O(3′) | 80.4(9) |
| Cu(1)—O(3) | 2.26(5) | N(1)—Cu(1)—O(3′) | 109.7(11) |
| Cu(1)—S(1) | 2.295(5) | N(1′)—Cu(1)—O(3′) | 81.8(11) |
| N(1)—C(2) | 1.24(4) | O(1)—Cu(1)—O(3) | 85.3(11) |
| N(1)—N(2) | 1.36(4) | N(1)—Cu(1)—O(3) | 75.4(15) |
| N(1)—H(2′C) | 0.8438 | N(1′)—Cu(1)—O(3) | 116.2(15) |
| N(1)—H(2′D) | 0.8555 | O(3′)—Cu(1)—O(3) | 34.7(17) |
| N(2)—C(1) | 1.30(5) | O(1)—Cu(1)—S(1) | 176.0(5) |
| N(2)—H(2) | 0.8600 | N(1)—Cu(1)—S(1) | 89.0(5) |
| N(2)—H(2′C) | 0.5968 | N(1′)—Cu(1)—S(1) | 89.2(4) |
| N(3)—C(1) | 1.30(5) | O(3′)—Cu(1)—S(1) | 103.5(8) |
| N(3)—H(3A) | 0.8600 | O(3)—Cu(1)—S(1) | 98.4(11) |
| N(3)—H(3B) | 0.8600 | C(2)—N(1)—N(2) | 114(2) |
| N(4)—C(7) | 1.38(4) | C(2)—N(1)—Cu(1) | 137(2) |
| N(4)—C(3) | 1.38(4) | N(2)—N(1)—Cu(1) | 108.5(16) |
| N(4)—H(4) | 0.8600 | C(2)—N(1)—H(2′C) | 101.6 |
| N(5)—O(4) | 1.22(5) | N(2)—N(1)—H(2′C) | 16.4 |
| N(5)—O(5) | 1.23(7) | Cu(1)—N(1)—H(2′C) | 117.0 |

**Table S3** Selected bond lengths (Å) and angles (°) for complex **2**.

| Bond names | Bond length(Å) | Bond angle | Angle(°) |
|---|---|---|---|
| Zn(1)—S(1) | 2.347(6) | O(1)—Zn(1)—S(1) | 162.2(5) |
| Zn(1)—O(1) | 1.987(11) | O(1)—Zn(1)—O(2) | 81.4(5) |
| Zn(1)—O(2) | 2.072(16) | O(1)—Zn(1)—O(3) | 92.5(5) |
| Zn(1)—O(3) | 2.045(18) | O(1)—Zn(1)—N(3) | 85.7(6) |
| Zn(1)—N(3) | 2.18(2) | O(2)—Zn(1)—S(1) | 98.7(4) |
| S(1)—C(1) | 1.70(3) | O(2)—Zn(1)—N(3) | 139.9(7) |
| O(1)—C(4) | 1.28(2) | O(3)—Zn(1)—S(1) | 105.1(3) |
| O(3)—N(5) | 1.24(2) | O(3)—Zn(1)—O(2) | 97.1(7) |
| O(4)—N(5) | 1.21(2) | O(3)—Zn(1)—N(3) | 121.4(7) |
| O(5)—N(5) | 1.22(2) | N(3)—Zn(1)—S(1) | 83.0(4) |
| O(6)—N(6) | 1.24(2) | C(1)—S(1)—Zn(1) | 98.5(5) |
| O(7)—N(6) | 1.24(2) | C(4)—O(1)—Zn(1) | 130.8(13) |

| | | | |
|---|---|---|---|
| O(8)—N(6) | 1.273(19) | N(5)—O(3)—Zn(1) | 118.3(16) |
| N(1)—C(1) | 1.31(2) | N(2)—N(3)—Zn(1) | 113.2(12) |
| N(2)—N(3) | 1.388(18) | C(2)—N(3)—Zn(1) | 130.2(15) |

**Table S4** Inhibitory rates (%) of **H-L** and complexes **1-3** towards seven selected tumour cell lines for 48 h.

| | **SKOV-3** | **BEL7404** | **Hela** | **Hep-G2** | **MGC-803** | **HL-7702** |
|---|---|---|---|---|---|---|
| **L** | 15.45±5.5 | 5.34±7.5 | 10.45±5.3 | 12.43±6.4 | 19.33±6.1 | 32.05±1.39 |
| **1** | 59.52±1.3 | 37.78±1.7 | 59.60±2.3 | 49.67±4.5 | 74.68±1.3 | 30.05±0.84 |
| **2** | 30.40±2.2 | 60.07±2.3 | 37.03±1.1 | 27.28±3.7 | 19.01±5.7 | 29.08±0.79 |
| **3** | 24.18±1.5 | 48.46±3.9 | 46.25±3.6 | 18.96±1.6 | 35.56±3.3 | 58.36±1.07 |

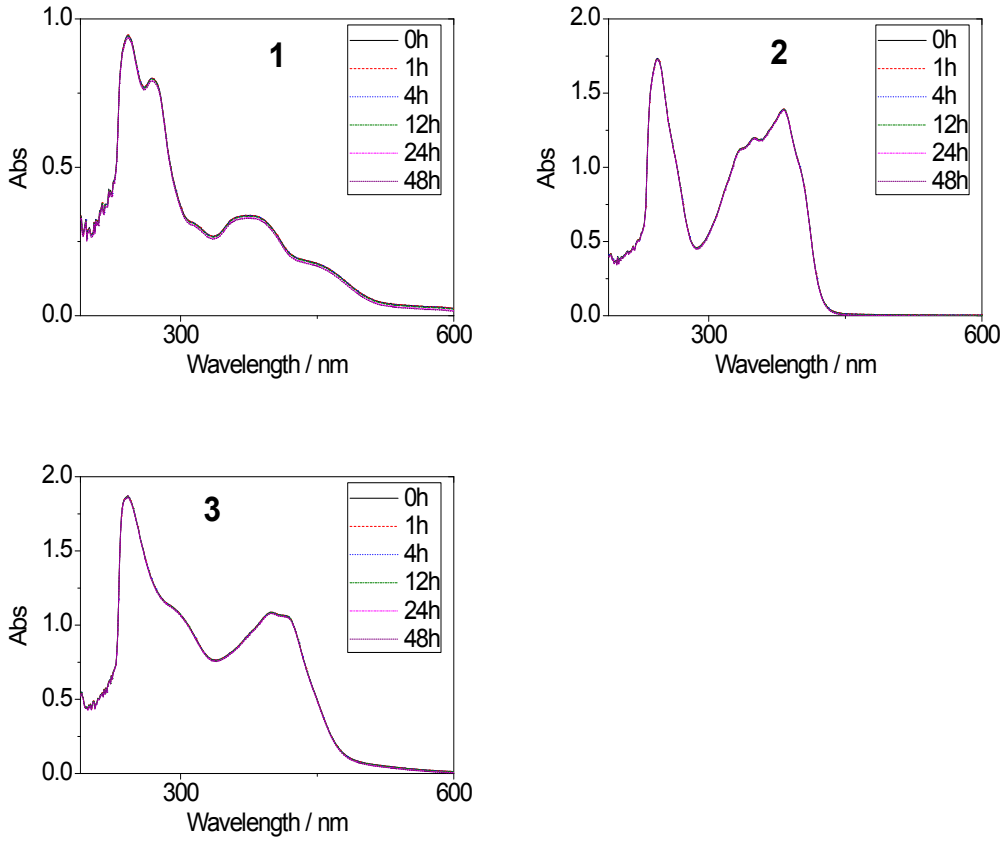


**Fig. S1**.Time-dependent stability studies on complexes **1-3** in PBS monitored by UV-vis absorption spectra.

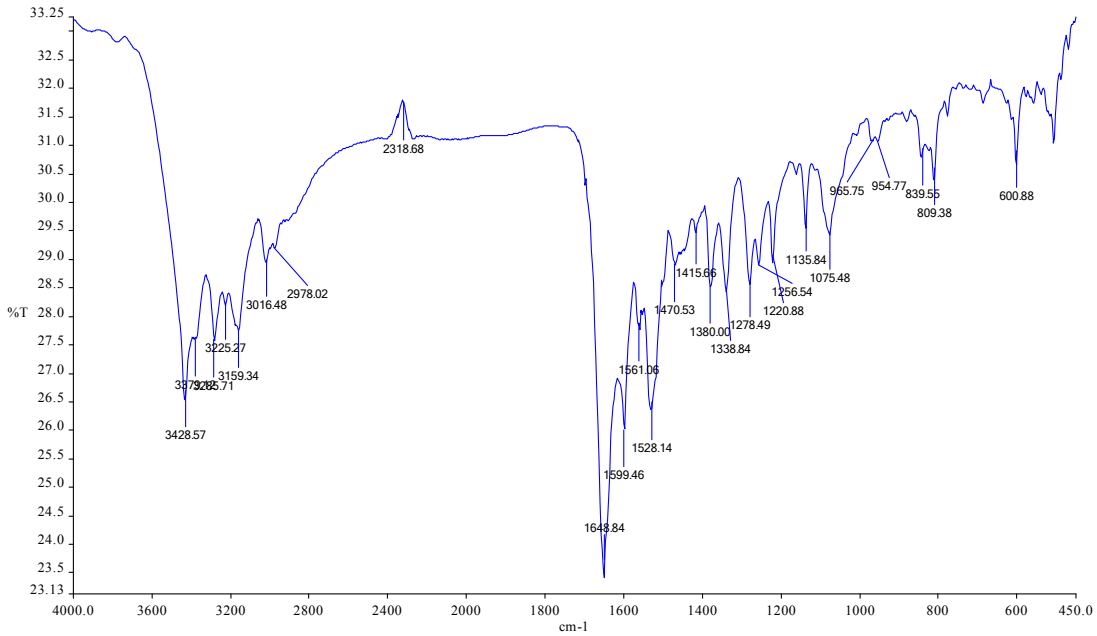


**Fig. S2.** IR of ligand **H-L**.

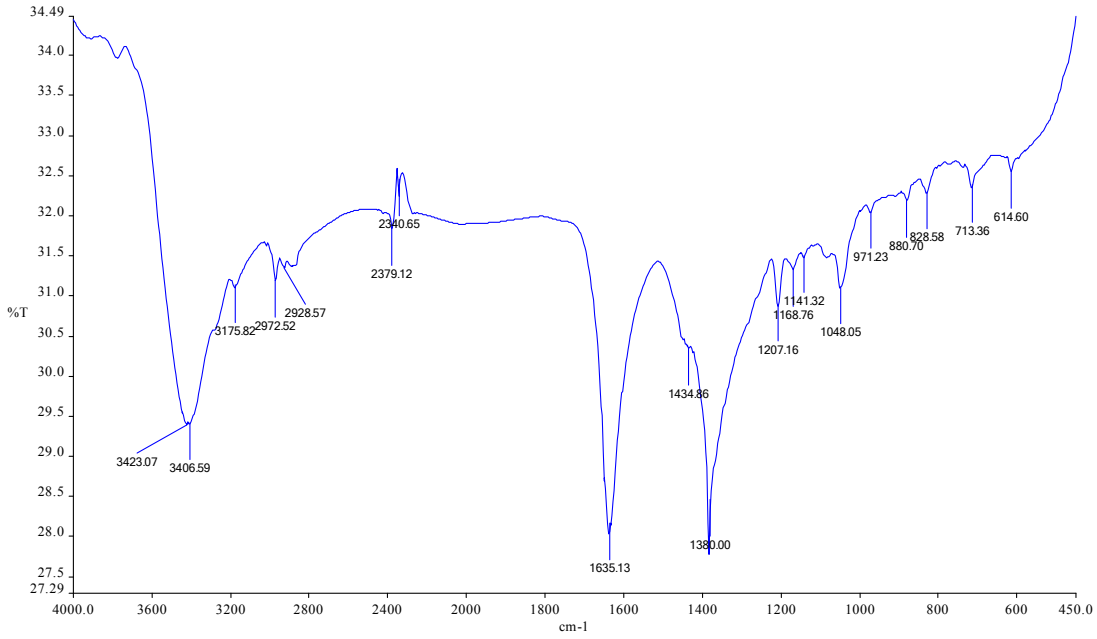


**Fig. S3.** IR of complex **1**.

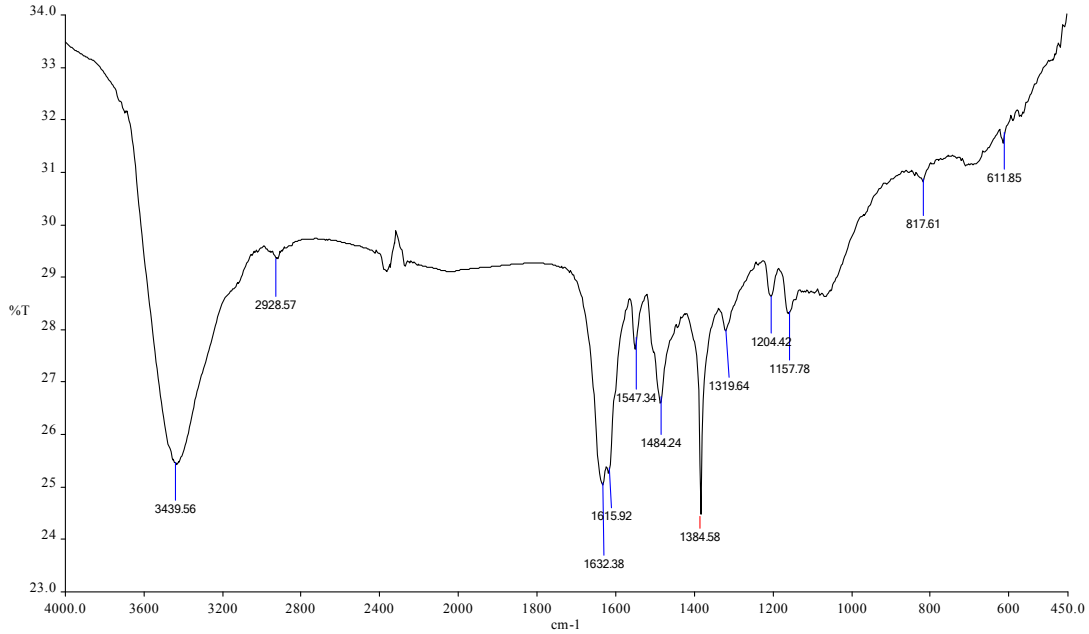


**Fig. S4.** IR of complex **2**.

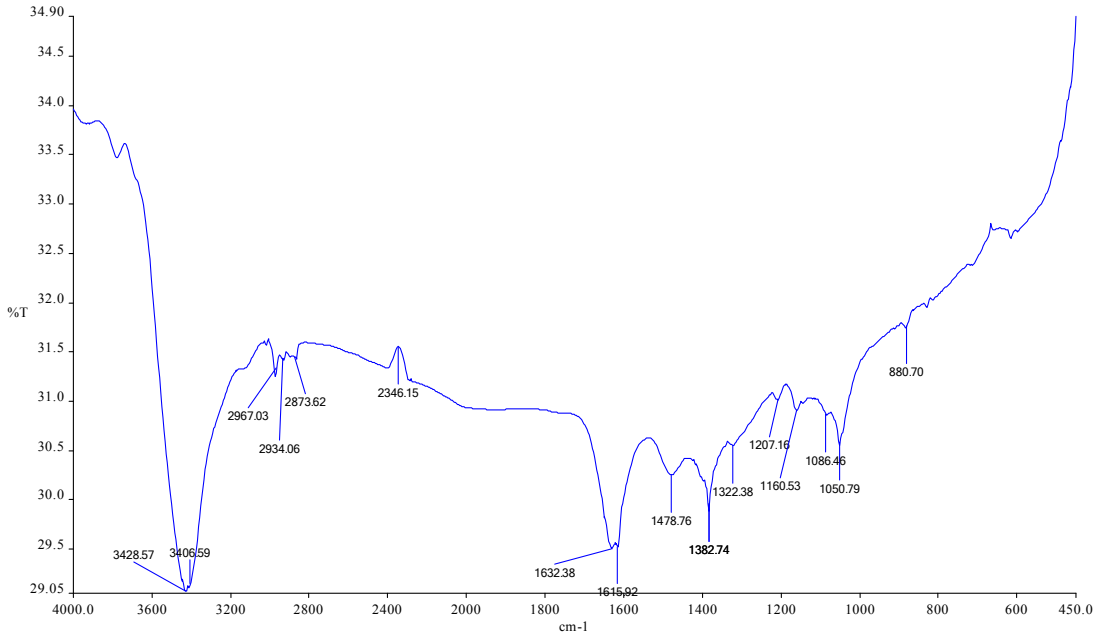


**Fig. S5.** IR of complex **3**.

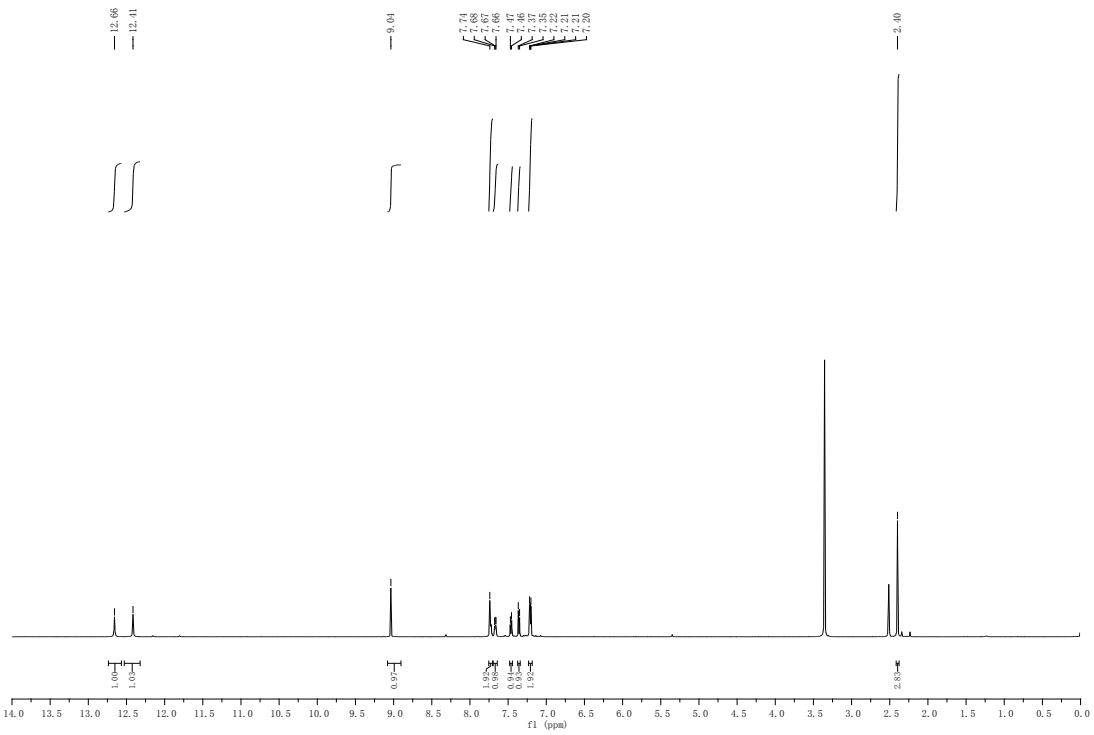


**Fig. S6.** $^{1}$H NMR of ligand **H-L**.

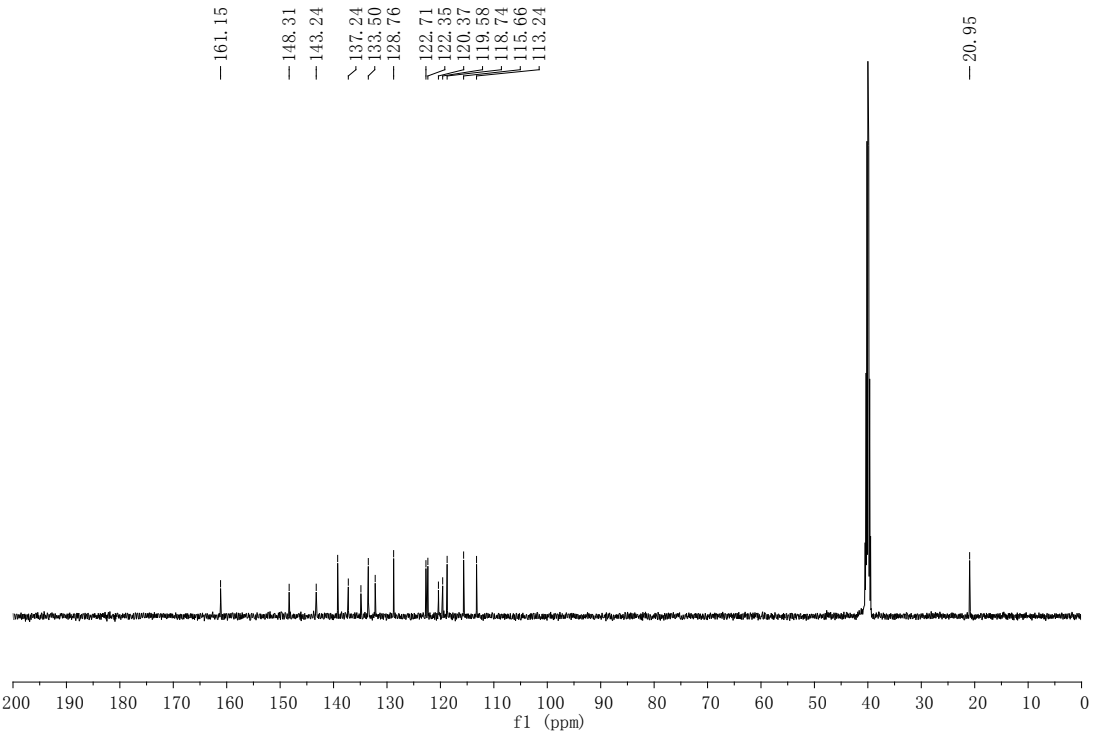


**Fig. S7.** $^{13}$C NMR of ligand **H-L**.

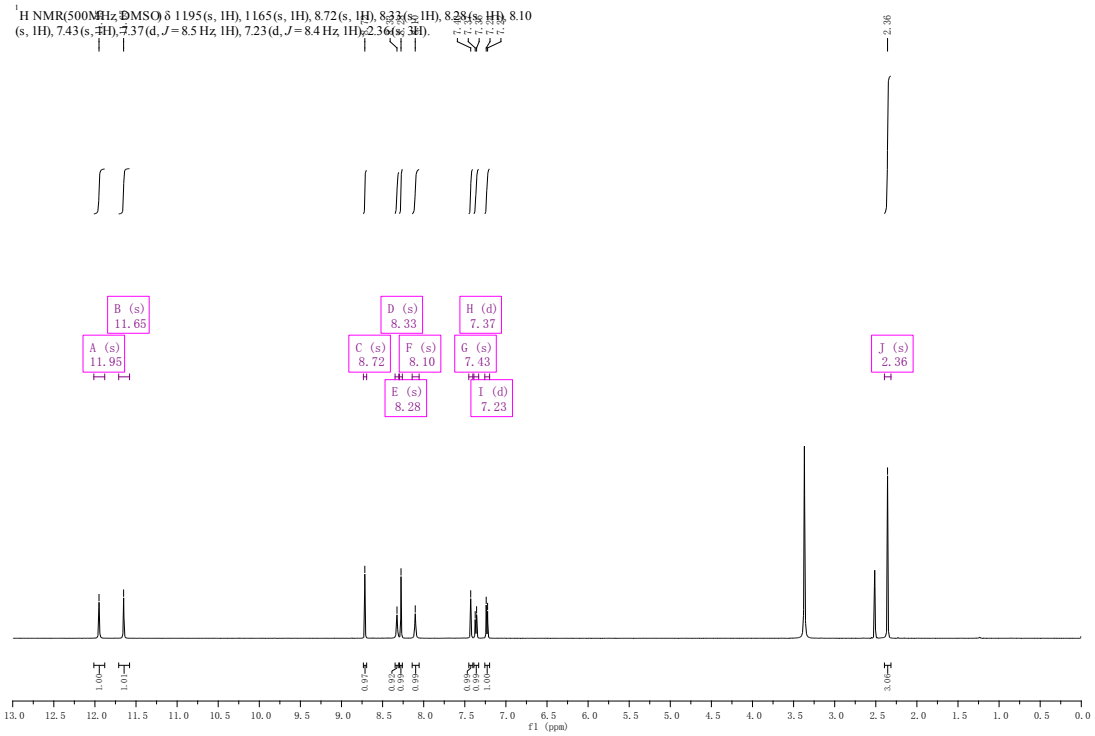


**Fig. S8.** $^{1}$H NMR of complex **2**.

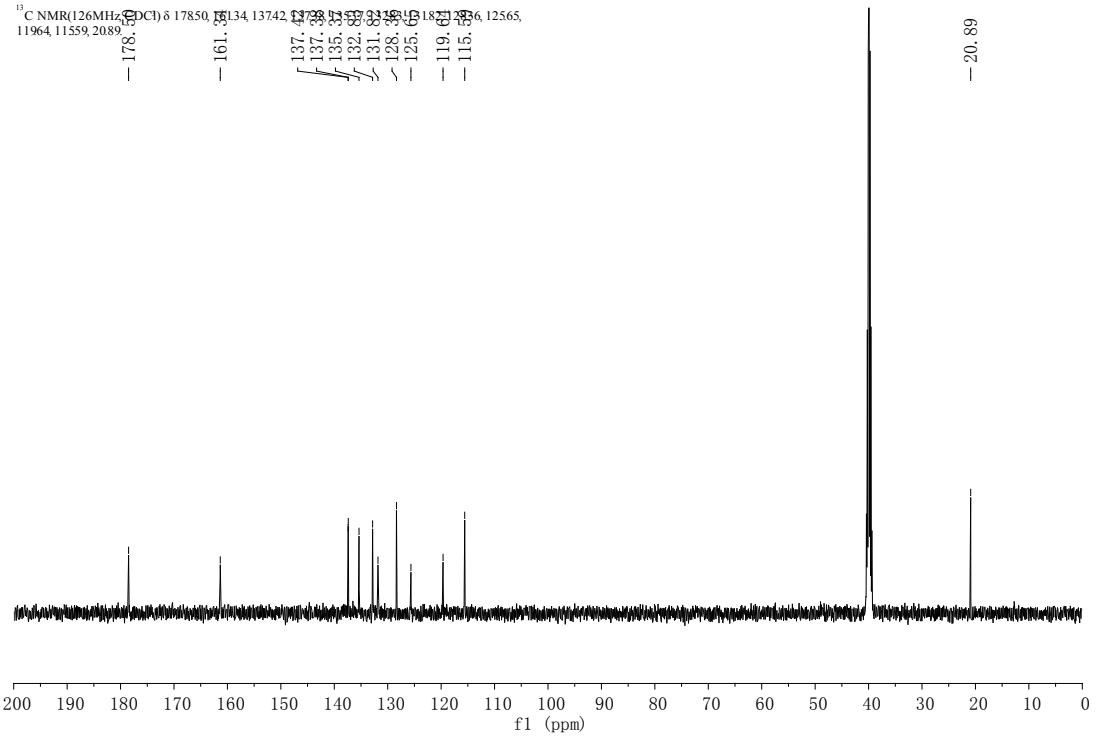


**Fig. S9.** $^{13}$C NMR of complex **2**.

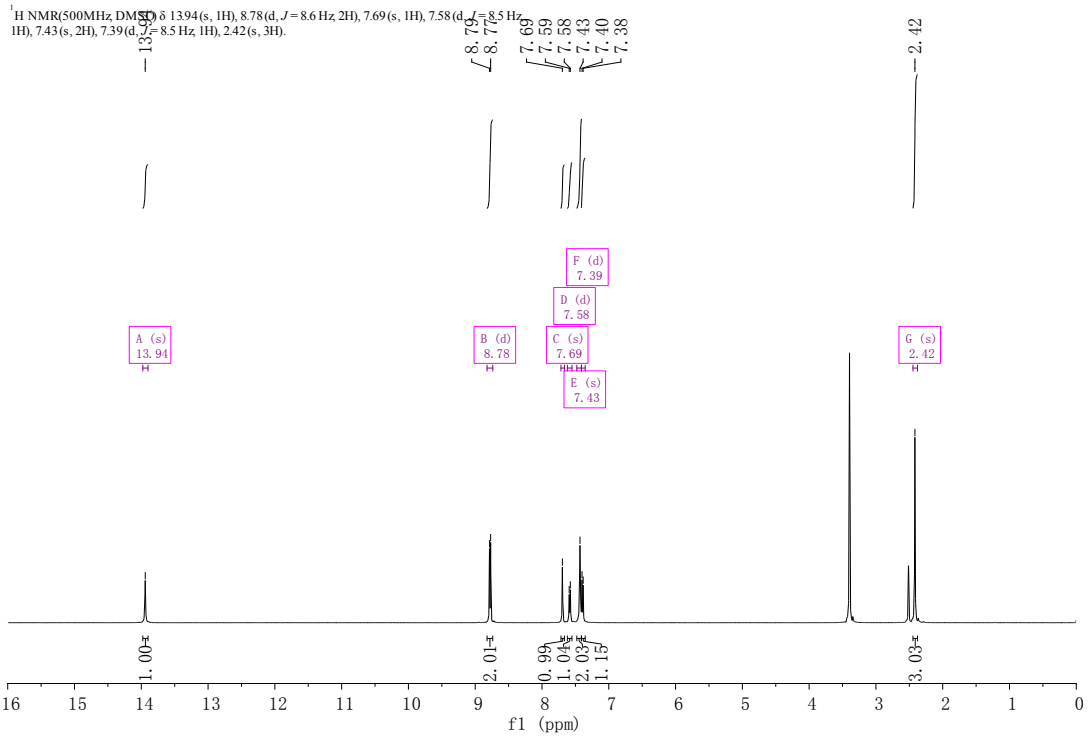


**Fig. S10.** $^{1}$H NMR of complex **3**.

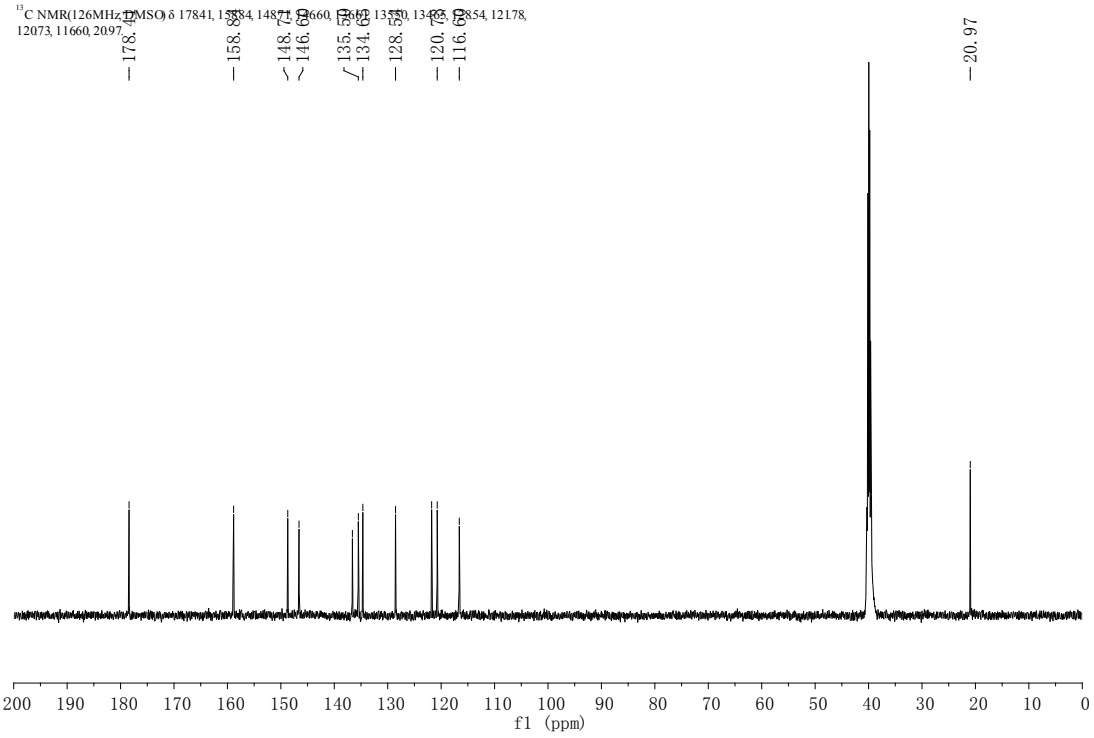


**Fig. S11.** $^{13}$C NMR of complex **3**.

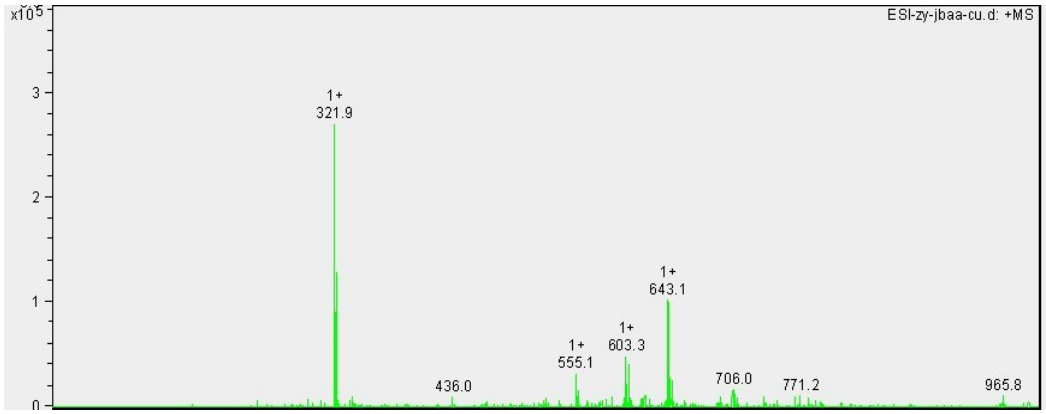


**Fig. S12.** MS of complex **1**.

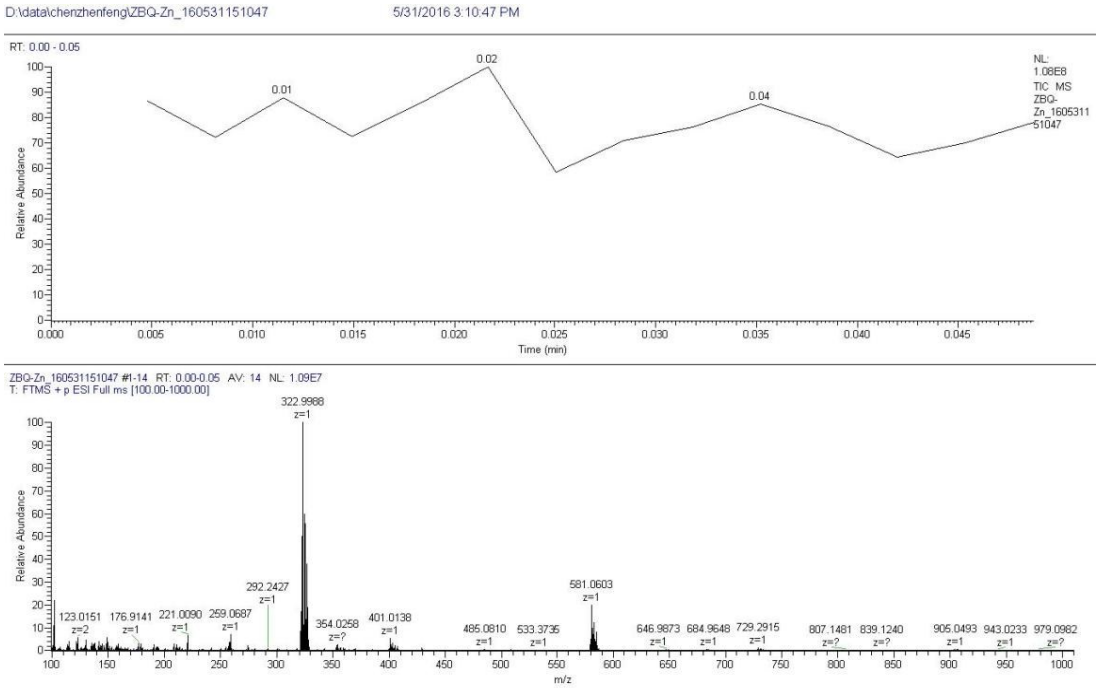


**Fig. S12.** MS of complex **2**.

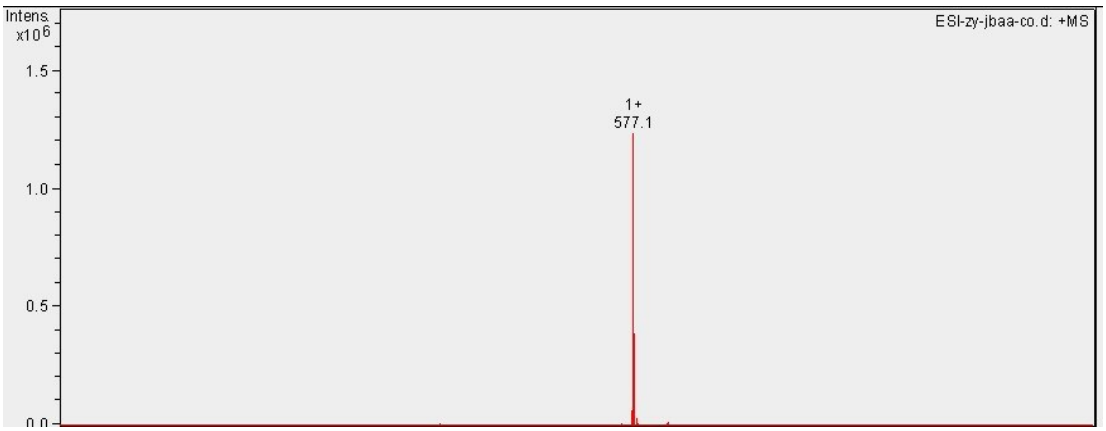


**Fig. S13.** MS of complex **3**.

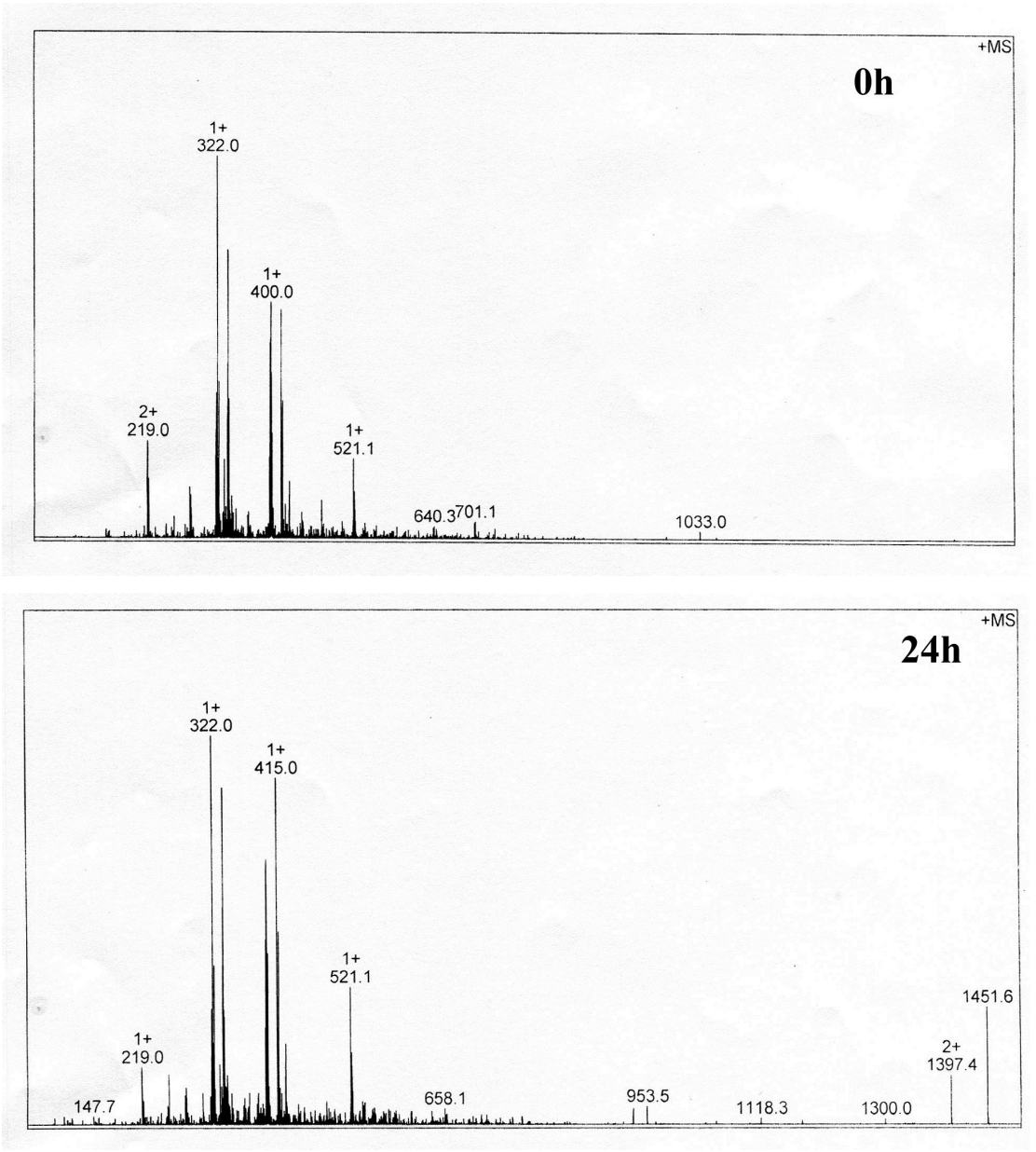


**Fig. S14.** The mass spectra of complex **1** in Tris-HCl buffer solution (containing 5% DMSO) for 0 h (top) and 24 h (down), respectively.

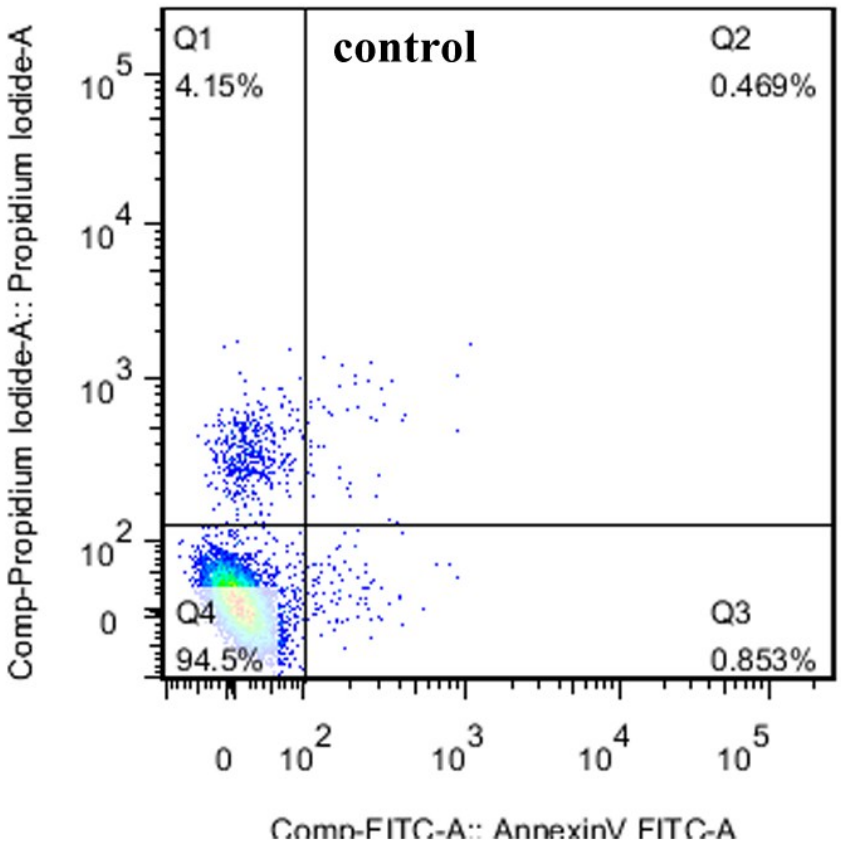
control
Q1
4.15%
Q2
0.469%
Q4
94.5%
Q3
0.853%
Comp-Propidium Iodide-A:: Propidium Iodide-A
Comp-FITC-A:: AnnexinV FITC-A
0
10^2
10^3
10^4
10^5

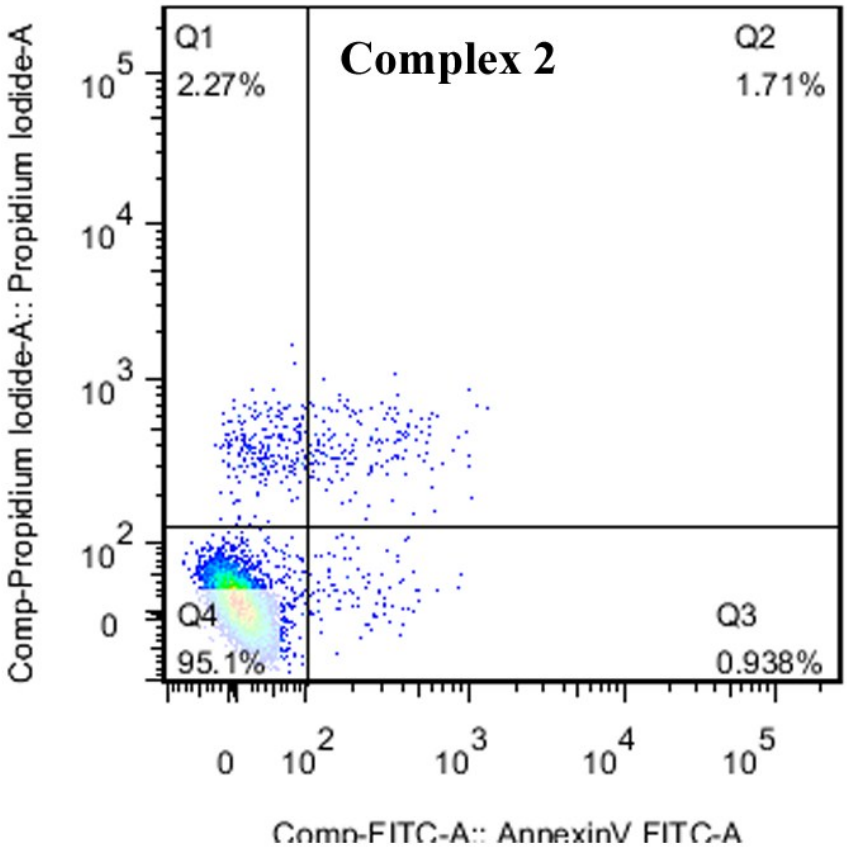
Complex 2
Q1
2.27%
Q2
1.71%
Q4
95.1%
Q3
0.938%
Comp-Propidium Iodide-A:: Propidium Iodide-A
Comp-FITC-A:: AnnexinV FITC-A
0
10^2
10^3
10^4
10^5

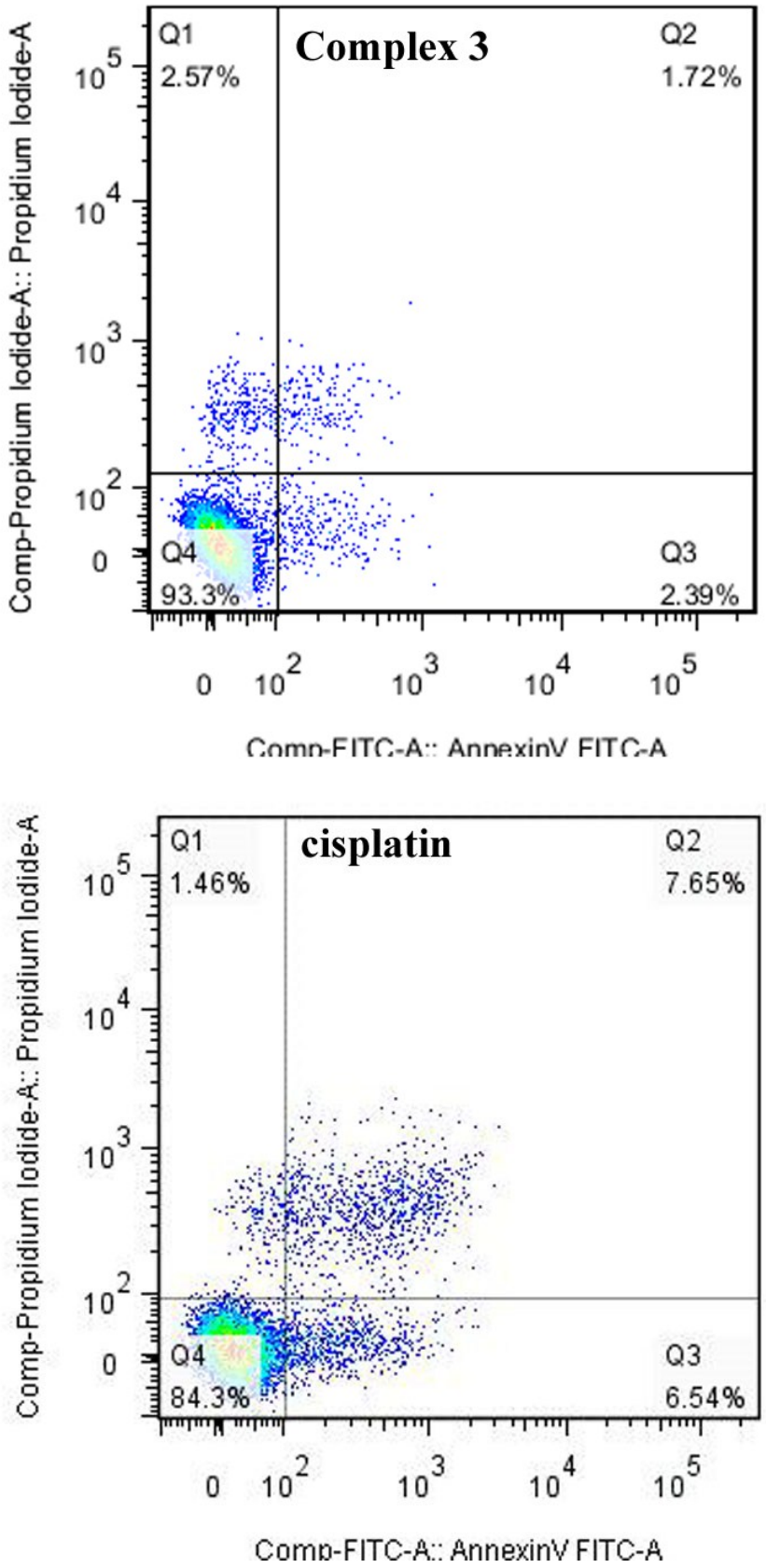


**Fig. S15.** Apoptosis of MGC80-3 cells treated with **2** (10 $\mu$M), **3** (10 $\mu$M) and cisplatin (10 $\mu$M) for 24 h, comparing with the control group cells.

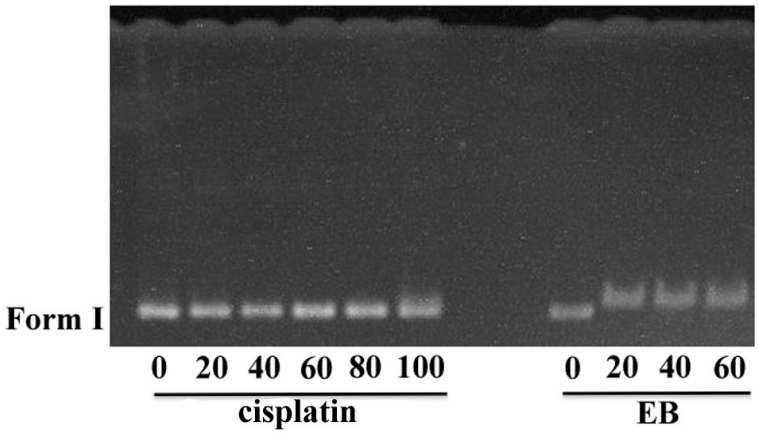


**Fig. S16.** Gel electrophoresis mobility shift assay of PBR322 DNA treated with cisplatin and EB (each compound with increasing concentrations of 20, 40, 60, 80 and 100 μM), respectively.

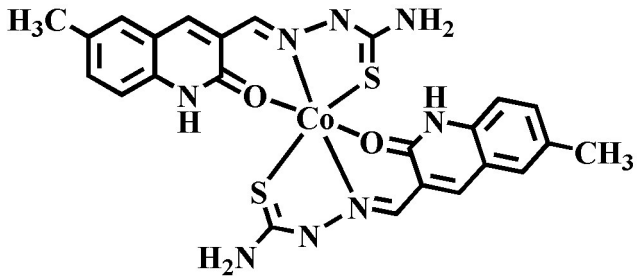


**Fig. S17.** Chemical structure of complex **3**.

**Experimental methods**

**Copper complex 1 induced $Ca^{2+}$ Fluctuation.** The level of intracellular free $Ca^{2+}$ was decided by using a fluorescent dye Fluo-3 AM which can across the MGC80-3 cell membrane and be cut into Fluo-3 by intracellular esterase. The Fluo-3 can specifically combine with the $Ca^{2+}$ and has a strong fluorescence with an excitation wavelength of 488.0 nm. After exposed to copper(II) complex **1** (10.0 $\mu$M), the MGC80-3 cells were harvested and washed twice with PBS, then resuspended in Fluo-3 AM (5.0 μM) for 30.0 min in dark. Detection of intracellular $Ca^{2+}$ was carried by Flow cytometer at 525.0 nm excitation wavelength.

**Copper complex 1 induced the loss of Δψ in MGC80-3 cells.** Depolarization of mitochondrial membrane potential (Δψ) for cell apoptosis results in the loss of JC-1 (5,5′,6,6′-tetrachloro-1,1′,3,3′-tetraethylbenzimidazolylcarbocyanine) staining from the mitochondria and a decrease in intracellular fluorescence intensity. After 24.0 h treatment with or without copper complexes **1** (10 μM), the MGC80-3 cells were harvested and washed twice in cold PBS, then resuspended in JC-1 staining (5 μg/mL) for 20-30 min in dark, and examined by flow cytometry.[1–8] The emission fluorescence for JC-1 was monitored at 590 nm, under the excitation wavelength at 488 nm.

**Assessment on the caspase-3 and caspase-9 activation for MGC80-3 cell apoptosis.** The measurement of caspase-3 and caspase-9 activity was performed by CaspGLOW Fluorescein Active Caspase-3 and caspase-9 Staining Kit.[1–8] $1\times10^6$ of MGC80-3 cells were cultured for 24.0 h. After a treatment with copper complex **1** (10

μM) for 24 h, these MGC80-3 cells were harvested and washed 5 times with cold PBS and were then mixed with 500 μL culture. 1.0 μL of FITC-DEVD-FMK or FITC-LEHD-FMK was consequently added and incubated for 2.0 h at 37 ℃ with 5% $CO_2$. The MGC80-3 cells were then examined by a FACSAria II flow cytometer equipped with a 488 nm argon laser and results were represented as the percent change on the activity in comparing with the control cells.

**Reactive oxygen species (ROS) levels detection.** DCFH-DA is a freely permeable tracer specific for ROS. DCFH-DA can be deacetylated by intracellular esterase to the non-fluorescent DCFH which is oxidized by ROS to the fluorescent compound 2',7'-dichloro florescein (DCF). Thus, $1.0\times10^6$ cells were exposed to copper complex **1** (10 μM) for 24 h, and 1.0 mM $H_2O_2$ used as a positive control of ROS production. After the exposure, these MGC80-3 cells were harvested, washed once with ice-cold PBS and incubated with DCFH-DA (100.0 μM in a final concentration) at 37 ℃ for 20-30 min in the dark. Finally, the MGC80-3 cells were washed again and maintained in 1.0 mL PBS. Finally, the ROS generation was assessed from these cells each sample by FACSAria II flow cytometer with excitation and emission wavelengths of 488.0 and 530.0 nm, respectively.[1–10]

**Western blotting.** The MGC80-3 cells harvested from each well of the culture plates were lysed in 150 μL of extraction buffer consisting of 149.0 μL of RIPA Lysis Buffer and 1.0 μL PMSF (100.0 mM). The suspension was centrifuged at 10000 rpm at 4.0 °C for 10.0 min, and the supernatant (10.0 μL for each sample) was loaded onto 10% polyacrylamide gel and then transferred to a microporous polyvinylidene

difluoride (PVDF) membrane. Western blotting was performed using anti-cytochrome c, anti-apaf-1, anti-bax, anti-bcl-2 and anti-β-actin antibody and horseradish peroxidase-conjugated antimouse or antirabbit secondary antibody. Protein bands were visualized using chemiluminescence substrate.

**References**

[1] Q.-P. Qin, J.-L. Qin, T.-M., G.-A. Yang, Z.-Z. Wei, Y.-C. Liu, H. Liang, Z.-F. Chen, *Sci. Rep.*, **2016**, 6, 37644; *doi: 10.1038/srep37644*.

[2] Y.-L. Li, Q.-P. Qin, Y.-C. Liu, Z.-F. Chen, H. Liang, J. Inorg. Biochem., **2014**, 137, 12-21.

[3] Z.-F. Chen, Q.-P. Qin, J.-L. Qin, Y.-C. Liu, K.-B. Huang, Y.-L. Li, T. Meng, G.-H. Zhang, Y. Peng, X.-J. Luo, H. Liang, *J. Med. Chem.* **2015**, *58*, 2159–2179.

[4] A. Prokop, J. A. Czaplewska, M. Clausen, M. König, A. Wild, R. Thorwirth, B. Schulze, K. Babiuch, D. Pretzel, U. S. Schubert, M. Gottschaldt, *Eur. J. Inorg. Chem.* **2016**, 3480–3488.

[5] J.-L. Qin, Q.-P. Qin, Z.-Z. Wei, C.-C. Yu, T. Meng, C.-X. Wu, Y.-L. Liang, H. Liang, Z.-F. Chen, *Eur. J. Med. Chem.* **2016**, *124*, 417−427.

[6] Q.-P. Qin, J.-L. Qin, T. Meng, W.-H. Lin, C.-H. Zhang, Z.-Z. Wei, J.-N. Chen, Y.-C. Liu, H. Liang, Z.-F. Chen, *Eur. J. Med. Chem.* **2016**, *124*, 380−392.

[7] T. Meng, S.-F. Tang, Q.-P. Qin, Y.-L. Liang, C.-X. Wu, C.-Y. Wang, H.-T. Yan, J.-X. Dong, Y.-C. Liu, *Med. Chem. Commun.* **2016**, *7*, 1802−1811.

[8] C.-C. Chou, J.-S. Yang, H.-S. Lu, S.-W. Ip, C. Lo, C.-C. Wu, J.-P. Lin, N.-Y. Tang, J.-G. Chung, M.-J. Chou, Y.-H. Teng, D.-R. Chen, *Arch. Pharm. Res.* **2010**, *33*,

1181–1191.

[9] F. Carvallo-Chaigneau, C. Trejo-Solis, C. Gomez-Ruiz, E. Rodriguez-Aguilera, L. Macias-Rosales, E. Cortes-Barberena, C. Cedillo-Pelaez, I. Gracia-Mora, L. RuizAzuara, V. Madrid-Marina, F. Constantino-Casas, Biometals **2008**, 21, 17–28.

[10] H.-H. Zou, L. Wang, Z.-X. Long, Q.-P. Qin, Z.-K. Song, T. Xie, S.-H. Zhang, Y.-C. Liu, B. Lin, Z.-F. Chen, Eur. J. Med. Chem. **2016**, 108, 1–12.